2023 IEEE International Conference on Robotics and Automation (ICRA 2023)
May 29 - June 2, 2023. London, UK

Towards Open-Set Material Recognition using Robot Tactile Sensing

Kunhong Liu, Qianhui Yang, Yu Xie, Xiangyi Huang

Abstract—**The texture recognition can provide clues for robots to interact with the external environment. The traditional tactile material recognition task is studied under the close-set assumption, which means that all types of materials are included in the training set. However, the open-set materials recognition for robots is of much greater significance because in the real-world applications, there is usually something that doesn't belong to any known class. Up to now, there is no researcher to further the discussion of this problem. To cope with unknown classes, this study proposes the Open set Material Recognition (OpenMR) based on General Convolutional Prototype Learning (GCPL). To handle the open space risk for GCPL caused by the lack of unknown samples in the training stage, we use Generative Adversarial Networks (GAN) to synthesize open-set samples as unknowns. The proposed framework is implemented and tested on two batches of tactile data collected in different exploratory motions on 8 material textures using the electronic skin. Compared with other open-set classifiers, experiments reveal that the proposed framework achieves competitive performance in both known classification and unknown detection.**

I. Introduction

Tactile intelligence is a hot research topic, as it helps robots interact with the external environment. Despite that the great success has been achieved in tactile perception, most works are based on closed conditions. That is, assuming all unknown samples belong to one of the known classes. However, in the open world, robots would have to face uncontrollable conditions as there would exist some objects beyond robotic knowledge database. This situation brings a new challenge for tactile materials recognition, which aims to identify both the known classes and unknown classes simultaneously.

Unlike humans that always accept new information to update knowledge according to their will, currently, robots can only recognize the types of materials included in their dataset, and fail to identify samples belonging to completely unknown classes beyond their stored knowledge. In contrast, we consider that each unknown sample should be rejected by the model to perform further exploration. The information of unknowns is then stored and labeled by experts to update the robotic knowledge database. This process is substantial for incremental learning [1] of robots.

Based on this consideration, open set recognition (OSR) is the first step for robots to explore unknowns. Different from normal classification tasks, OSR requires that models should not only identify the samples of specified known classes, but also correctly reject unknowns (i.e. new classes absent in the training data) [2]. In Figure 1(a), the original dataset includes 4 known classes and 2 unknown classes (uk?5 and uk?6). Figures 1(b) and (c) show the decision boundaries drawn by the traditional and open set classifiers. In Figure 1(b), the samples from unknown classes are wrongly classified into known classes; instead, the open set classifier labels them as unknowns in Figure 1(c).

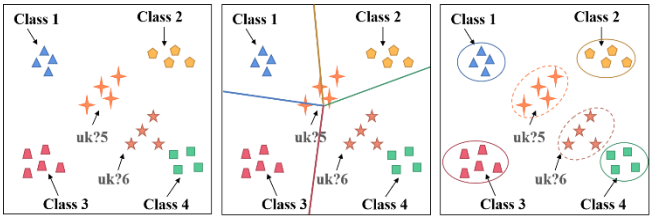

Figure 1. Comparisons of the traditional classification task and the OSR task. (a) The distribution of the original dataset; (b) The traditional classification task; (c) The OSR task.

The OSR task is more consistent with the real scenarios in the open world. For example, in autonomous driving [3], when encountering unconventional situations or objects that have never been seen before, the system is expected to issue warnings and return control to humans. The OSR task had also made great progress in many other fields such as face recognition [4, 5], object detection [6, 7], action localization [8], and semantic segmentation [9]. Recently, B. J. Meyer et al. [10] supposed that objects observed by robots beyond the training set distribution might affect their actions. Thus, they proposed an open set active learning approach that allowed a robotic vision system to extend its understanding of the environment beyond the original training distribution. To our knowledge, previous works [11-16] related to tactile material recognition mainly focused on the traditional close-set recognition task, without exploration to the OSR task.

Instead, for the first time, we step toward the open set materials recognition and propose a framework for Open-set Material Recognition (OpenMR for short) based on General Convolutional Prototype Learning (GCPL) [17]. Since unknowns can't be observed during training, GCPL still inevitably faces the open space risk. Therefore, we extend GCPL by deploying Generative Adversarial Networks (GAN) to generate open set samples that simulate unknowns, with the aim to promote the model to draw decision boundaries with wider margins among known and unknown classes.

In summary, the main contributions of this paper include:

- The robotic tactile material recognition is extended to the open set problem for the first time, and a framework OpenMR is designed to jointly recognize knowns accurately and detect unknowns effectively.

*This work was supported by National Natural Science Foundation of China (No. 61772023), National Key Research and Development Program of China (No. 2019QY1803), Fujian Science and Technology Plan Industry University Research Cooperation Project (No.2021H6015), and Open Fund of Hubei Key Laboratory of Mechanical Transmission and Manufacturing Engineering at Wuhan University of Science and Technology (MTMEOF2019A01). Corresponding author: Kunhong Liu (lkhqz@xmu.edu.cn) and Xie Yu (xieyu@xmu.edu.cn).

K. Liu is with the School of Film, Xiamen University, China. Q. Yang is with the School of Informatics, Xiamen University, China. Y. Xie and X. Huang are with the School of Aerospace Engineering, Xiamen University, China.

- Two batches of tactile data containing 8 classes are collected based on the tactile sensor under distinct settings.
- A new measure for evaluating the openness degree is proposed based on the *Dunn index* by the ratio of intra-class and inter-class distances among diverse classes.

II. Related Work

A. Robot Tactile Material Recognition

In [12], a set of tactile descriptors was designed to extract robust features from raw tactile signals, but such tactile descriptors are invariant only for particular exploration movements. In [11], authors deployed the relocation migration of sensors to acquire three data sets with increasing difficulty levels and designed a deep neural network to learn self-organizing features of raw tactile arrays. In [16], a novel Spatio-Temporal Attention Model was proposed to extract spatial features from tactile texture and the temporal correlation of tactile sequences. Although these works have obtained excellent performance on the close-set, in which the test environment is consistent with the training set, there is still a lack of exploration of the OSR problem that contains unknown classes in the real open world.

B. The OSR problem

A space far from known data is often considered *open space* $\mathcal{O}$, so labeling any sample in this space as known classes will bring a risk, as is called *open space risk* $\mathcal{R}_{\mathcal{O}}$ [18], calculated by formula (1).

$$\mathcal{R}_{\mathcal{O}}(f) = \frac{\int_{\mathcal{O}} f(x)dx}{\int_{\mathcal{S}_{\mathcal{O}}} f(x)dx} \tag{1}$$

where $\mathcal{S}_{\mathcal{O}}$ denotes the overall measure space, and f is the measurable identification function. $f(x) = 1$ means that class x in the known class set is recognized, otherwise $f(x) = 0$. The more samples in the open space $\mathcal{O}$ are labeled as known classes, the larger is the value of $\mathcal{R}_{\mathcal{O}}$.

Let C_{TR}, C_{TE} represent the sets of classes used in training and test sets respectively, and $|\cdot|$ denote the number of classes in the corresponding set. The *openness* index [19] of the recognition task reflects the difficulty level of the OSR problem, as given by formula (2).

$$openness = 1 - \sqrt{\frac{|C_{TR}|}{|C_{TE}|}} \tag{2}$$

A larger *openness* value indicates that more unknown classes are involved. If there are no new classes in the testing phase, i.e. $|C_{TR}| = |C_{TE}|$, it is equivalent to the traditional close-set problem and the *openness* equals 0.

Based on OpenMax [20], Classification Reconstruction learning for Open Set Recognition (CROSR) [21] was proposed to tackle unknown class detection using reconstructed latent representations. In [19], an encoder-decoder model trained with adversarial loss was used to generate counterfactual images. In [22], Conditional Gaussian Distribution Learning (CGDL) learned conditional gaussian distributions by driving different latent features to approximate different gaussian models to well reject unknown classes. Recently, [23] proposed to learn placeholders for OSR, transforming closed-set training into open-set training. [24] combined decisions reached by multiple one-vs-rest networks (OVRNs) to get the collective decision score, achieving the separation of unknowns. [25] revealed that the model trained with noisy negative images greatly improves open-set recognition. Although these methods performed well on the OSR tasks, they didn't consider the distributions of features extracted from known and unknown classes, leading to potential *open space risk*.

III. Methodology

In the OpenMR framework, prototype matching is deployed for known classification and unknown detection. The generator synthesizes open-set samples that are close to prototypes to fool the discriminator into identifying them as true samples. Thus, the generated open-set examples push away the prototypes of known classes to enhance unknown detection. The overall workflow is illustrated in Figure 2.

A. General Convolutional Prototype Learning

The excellent performance of convolutional neural networks (CNNs) makes them be widely used in computer vision and other fields [26]. However, in image classification, CNN with the Softmax layer is a pure discriminative model by dividing the whole feature space into multiple partitions and splitting the spatio-temporal features, leading to its poor rejection ability for adversarial examples. Consequently, CNN tends to assign the samples in unknown classes to some known classes with high confidence. Thus, it is hard to deal with the OSR problem using CNN alone.

In [17], Convolutional Prototype Learning (CPL) was proposed to combine prototype-based classifiers with CNN. It improved the accuracy in rejecting unknown classes by projecting samples to some specific feature subspace close to the prototype. A new prototype loss (PL) is added to CPL as regularization to make features of the same class more compact, called GCPL. In GCPL, each class maintains one or more prototypes, denoted as $M = \{m_{ij}\}$. Here $i \in \{1, 2, \cdots, C\}$ denotes the index of classes and $j \in \{1, 2, \cdots, K\}$ denotes the index of the prototypes in each class. Let θ be the parameters of the feature extractor. As for an input sample x, GCPL deploys CNN without the Softmax layer as a feature extractor $f(x; \theta)$ to extract discriminative features, and then assigns it to the class where the nearest prototype belongs to:

$$x \in class \quad \arg\max_{1 \le i \le C} g_i(x) \tag{3}$$

where $g_i(x)$ is the discriminant function for class i:

$$g_i(x) = -\min_{1 \le j \le K} \left\| f(x; \theta) - m_{ij} \right\|_2^2 \tag{4}$$

The prototype matching of sample x is based on the distance, so the probability of x belonging to the prototype m_{ij} is calculated by:

$$p\left(x \in m_{ij} | x\right) = \frac{e^{-\gamma d\left(f(x), m_{ij}\right)}}{\sum_{k=1}^{C} \sum_{l=1}^{K} e^{-\gamma d\left(f(x), m_{kl}\right)}} \tag{5}$$

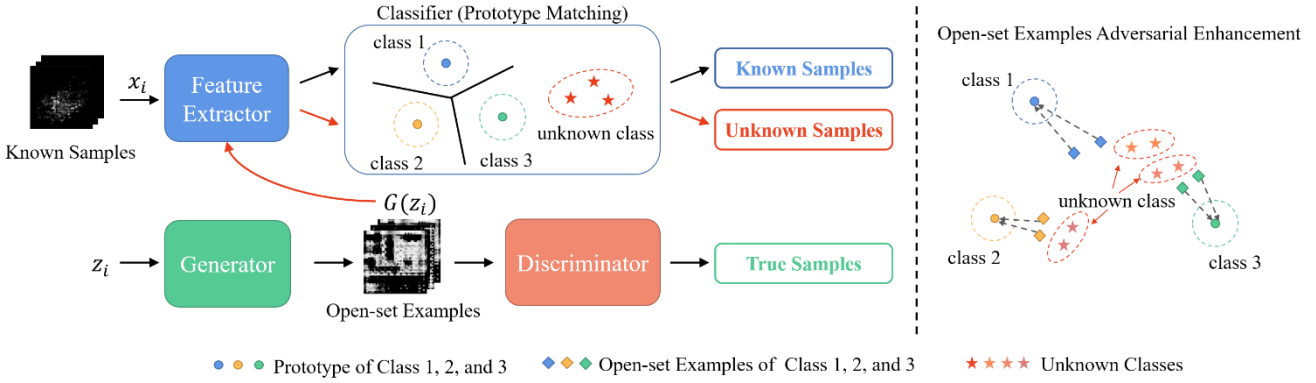

Figure 2. The overall structure of the proposed open-set material recognition framework.

where $d(f(x), m_{ij}) = \|f(x) - m_{ij}\|_2^2$ denotes the distance between $f(x)$ and m_{ij}, and γ is the hyper-parameter. Let m_{yj} be the closest prototype from the genuine class, then the probability of $p(y|x)$ is given by:

$$p(y|x) = \sum_{j=1}^{K} p(x \in m_{yj}|x) \tag{6}$$

Based on formula (6), the cross entropy loss is defined by:

$$l((x,y);\theta,M) = -\log p(y|x) \tag{7}$$

It is obvious that minimizing the cross entropy loss in formula (7) during training can decrease the distance between the samples with the prototypes which come from the genuine class of the samples. Furthermore, PL that can make features of the same class more compact is defined as:

$$pl((x,y);\theta,M) = \|f(x) - m_{yj}\|_2^2 \tag{8}$$

Let α be a weight hyperparameter, and the total loss in GCPL is given as follows:

$$l_1 = l((x,y);\theta,M) + \alpha pl((x,y);\theta,M) \tag{9}$$

Since the classification loss and the prototype loss emphasize the inter-class separable and intra-class compact respectively, GCPL is more suitable for the open-set recognition task. Therefore, our framework for the open-set materials recognition problem is designed based on GCPL.

B. The Open-set Examples Generation

GCPL can learn more compact intra-class boundaries, but it still cannot constrain the decision boundaries of classifiers among known and unknown classes due to the lack of information about unknowns during training. Given this, we design an open-set samples generation mechanism to supplement the knowledge of unknowns.

In Figure 2, the open-set samples generation mechanism consists of the generator G, the discriminator D, and the classifier C. Let $\{z_1, \cdots, z_M\}$ from a prior distribution $P_{pri}(z)$ and $\{x_1, \cdots, x_M\}$ denote the input samples. The generator maps a latent variable z from $P_{pri}(z)$ to produce outputs $G(z)$, and discriminator $D: \mathcal{X} \to [0,1]$ represents a probability that sample x is produced from a real or fake distribution. The generator is optimized to generate samples closer to the known classes, to deceive the discriminator by:

$$\max_G \frac{1}{M}\sum_{i=1}^{M}[\log D(G(z_i))] + \beta H(z_i, m_{yj}) \tag{10}$$

Then $G(z)$ is fed to the feature extractor to get the discriminative features $f(G(z))$, simplified as $f'(z)$. Let $S(\cdot)$ denote the Softmax function and β be a weight hyperparameter. $d(f'(z_i), m_{yj}) = \|f'(z_i) - m_{yj}\|_2^2$ denotes the distance between $f'(z_i)$ and m_{yj}. H is the information entropy function as given by:

$$H = -\frac{1}{M}\sum_{i=1}^{M} S(d(f'(z_i), m_{yj}))\log S\left(d(f'(z_i), m_{yj})\right) \tag{11}$$

Instead, the discriminator tries to distinguish the samples from the real and generated fake data sets:

$$\max_D \frac{1}{M}\sum_{i=1}^{M}\left[\log D(x_i) + \log\left(1 - D(G(z_i))\right)\right] \tag{12}$$

Maximizing the information entropy function in formula (10) would force the generator to synthesize samples closer to the prototype center of the known class, while formula (12) forces the discriminator to identify the synthetic fake samples. This adversarial mechanism is important for drawing decision boundaries among known and unknown classes. For the input samples from unknowns with higher differences from the knowns, the classification boundary of the classifier is generally sufficient to detect the unknowns.

However, if the unknown classes are similar to the knowns (such as the unknown class in Figure 2), and the GCPL trained only on the knowns lack the information of the unknown sample, the classifier tends to assign the unknowns that are relatively close to the prototype center of the known class. In this case, it is very effective to synthesize the open set samples to simulate unknown classes. In Figure 2, when the open set samples close to the knowns are utilized to enhance the training samples, the decision boundary of the classifier would be pushed to the region close to the knowns, so that the test samples from unknowns can be effectively detected even if they are very similar to the known class.

IV. Experimental Setup

A. Sensor Setup

We use electronic skin (Pressure Mapping Sensor 5076, Tekscan, USA) to obtain tactile data, as shown in Figure 3(a). In Figure 3(b), a tactile data collection unit is designed to attach the sensor to the end of the robotic arm. To enhance the imaging quality when the e-skin is in contact with the material, a double layer of foamed silicone rubber is added under the e-skin. The first layer is close to the e-skin, the shape is consistent with the e-skin, and the thickness is 5 mm. The second layer is a cylinder with a diameter of 25 mm and a thickness of 5 mm, the e-skin and double-layer foamed silicone rubber is pressed on the plane plate of an I-shaped structure to form a convex structure. Such a convex structure provides better contact and then reduces the vibration of the tactile data imaging caused by unstable control of the robotic arm's motion. A data acquisition card [27] is installed in the reserved space of the I-shaped structure, and is used to collect data at the acquisition frequency of 100 Hz. The tactile data collection unit is installed on a 6-DOF robotic arm (UR5, Universal Robots, Denmark). And 8 types of square sticks made of different materials are chosen, as shown in Figure 3(c). For exploration, the material is clamped with a bench vice, as shown in Figure 3(d).

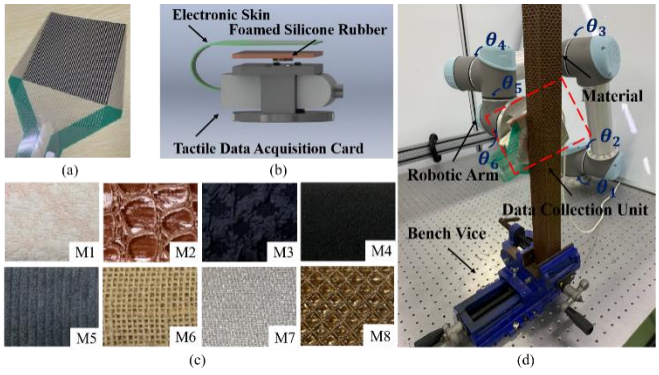

Figure 3. (a) The tactile sensor; (b) The tactile data collection unit; (c) The test materials: M1 *coarse towel*, M2 *crocodile pattern*, M3 *relief cloth*, M4 *sponge*, M5 *horizontal fabric*, M6 *linen*, M7 *gauze*, M8 *diamond pattern*; (d) The tactile data collection unit installed on the UR5 robotic arm collected data.

To simulate the data diversity brought by open scenes, we change the poses of the robotic arm before obtaining each batch of data. Firstly, we control the angles of robot joint θ_5 and θ_6 (see Figure 3(d)), since the joints closest to the end-effector (i.e. the data collection unit) have the greatest impact on the tactile data imaging. And then z is changed by the pose $P\ (x, y, z, R_x, R_y, R_z)$ of the end effector of the robotic arm. After adjusting these parameters, the data is collected again by pressing various materials. Let $f_{i,j}(t_k)$ be the force value reflected by the sensor unit in row i and column j at time t_k, and N and M represent the rows and columns of the e-skin. The force reflected by the e-skin is the sum of the force values of all the sensing points:

$$F(t_k) = \begin{bmatrix} f_{0,0}(t_k) & \cdots & f_{0,M}(t_k) \\ \vdots & \ddots & \vdots \\ f_{N,0}(t_k) & \cdots & f_{N,M}(t_k) \end{bmatrix} \tag{13}$$

To simplify the data collection process, the resultant force value embodied by the e-skin is used as its interaction force in contact with the material.

We collect 8 classes of tactile data based on the tactile sensor, and the data collection process is given as follows:

1) *Batch 1:* The robotic arm presses the middle area of the material for exploring. Each time the e-skin is in contact with the material, a frame of tactile sample is recorded. Four forces are applied to press the material: 2 N, 5 N, 7 N, and 10 N.

2) *Batch 2:* The robotic arm presses the bottom area of the material with an initial force of nearly 10N and then slides upward at a constant velocity for 2 seconds from the bottom. Each sample contains 200 frames of tactile information. Given the high similarity between adjacent frames, we take a tactile image every 50 frames. Data is collected at four speeds: 2 cm/s, 4 cm/s, 6 cm/s and 8 cm/s.

B. The Analysis of Dataset

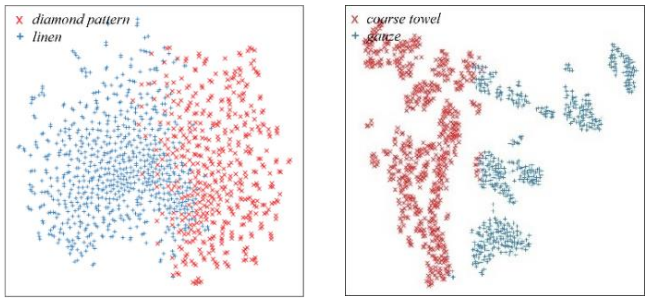

Figure 4. Cluster distributions: (a) The clustering results of *linen* and *diamond pattern* in the same batch. (b) The clustering results of *coarse towel* and *gauze* in the same batch.

In Figure 4, the clustering method is applied to explore feature distribution from different classes. The features of *diamond pattern* and *linen* are close to each other in cluster distribution and even overlap in some samples in Figure 4(a). A similar situation also appears between *coarse towel* and *gauze* in Figure 4(b). This reveals that in the data distributions, samples in these two classes tend to be misclassified to each other, and thus reduce the performance of classifiers. Moreover, the poor separation among different classes means that the OSR task is more difficult and complex because some unknown classes that appear in the test data may be misclassified to known classes. To better quantitatively analyze the separation of different classes and the intra-class compact of the same class, the *Dunn index* [28] is adopted to evaluate the difficulty level of the classification task. The formula of the *Dunn index* is given by:

$$D = \frac{\min\limits_{1 \le k \le k' \le m} d_{min}(C_k, C_{k'})}{\max\limits_{1 \le l' \le m} diam(C_{l'})} \tag{14}$$

where m is the number of clusters, and $d_{min}(C_k, C_{k'})$ measures the degree of dispersion between any two clusters C_k and $C_{k'}$. $diam(C_{l'})$ measures the intra-class distance within class $C_{l'}$. Therefore, the smaller *Dunn index* indicates the higher difficulty level of the OSR task.

Based on formula (14), we calculate the *Dunn index* between every class pair. TABLE I shows that the *Dunn*

indices of different class pairs vary greatly, meaning that the difficulty of the OSR task varies across different classes in the training set.

TABLE I. THE DUNN INDEX BETWEEN EVERY TWO CLASSES

	M1	M2	M3	M4	M5	M6	M7	M8
M1	-	4.57	2.21	2.07	3.65	3.68	2.90	5.32
M2	-	-	4.03	3.14	3.71	9.28	5.28	13.33
M3	-	-	-	2.67	1.97	5.00	3.03	3.66
M4	-	-	-	-	1.86	3.20	2.24	3.18
M5	-	-	-	-	-	3.00	2.74	4.12
M6	-	-	-	-	-	-	4.87	8.20
M7	-	-	-	-	-	-	-	5.13

Since different classes contribute differently to the difficulty of the OSR task, the *openness* index should reflect this distinction. Therefore, we extend the formula of *openness* in (2) by reweighting the *Dunn index* between unknown classes in the test set and known classes in the training set. Formula (2) is rewritten as:

$$openness = 1 - \sqrt{\frac{|C_{TR}|}{|C_{TE_k}| + \sum_{i=1}^{|C_{TE_{uk}}|} \frac{\mu}{D_i}}} \tag{15}$$

where μ is the mean value of D_i in the set of unknowns:

$$\mu = \frac{\sum_{i=1}^{|C_{TE_{uk}}|} D_i}{|C_{TE_{uk}}|} \tag{16}$$

Let C_{TE_k} and $C_{TE_{uk}}$ represent the set of known classes and unknown classes used in the test set respectively. In general, C_{TE_k} equals $|C_{TR}|$. D_i is the mean value of the *Dunn index* calculated between the i^{th} unknown class in the set of $C_{TE_{uk}}$ and each known class in the set of C_{TE_k}.

V. EXPERIMENTAL RESULTS AND DISCUSSIONS

Data setting. Following the setting in [19, 22], we select some classes randomly from the *Batch* 1 data to use them as known classes, and the remainder classes are used as unknowns. We split the known classes data into the training and validation sets at a 4:1 proportion, and the unknown data is treated as the test data. To explore the robustness of the proposed method under different *openness*, the number of known classes in training is fixed and the number of unknowns gradually increases. The specific division of classes in the training and test data are given as follows:

1) E5: 5 classes (*M1*, M3, *M4*, *M5*, and *M6*) are randomly selected as the training set, and *M2*, *M7*, and *M8* are the unknown classes. Furtherly, the number of unknown classes is increased from 1 to 3 by the setting of *E5-1*, *E5-2*, and *E5-3* with the *openness* of 8.7%, 16.1%, and 21.6% respectively.

2) E4: 4 classes data (*M1*, *M4*, *M6*, and *M7*) are randomly selected as the training set. And *M2*, *M3*, *M5*, and *M8* are the unknown classes. The number of unknown classes is increased from 1 to 4 in the setting of *E4-1*, *E4-2*, *E4-3*, and *E4-4* with the *openness* of 10.6%, 19.4%, 25.8%, and 30.9% respectively.

3) E3: 3 classes (*M2*, *M4*, and *M7*) are randomly selected as the training set. And *M1*, *M3*, *M5*, *M6*, and *M8* are selected as the unknown classes. Besides, the number of unknown classes is increased from 1 to 5 in the setting of *E3-1*, *E3-2*, *E3-3*, *E3-4*, and *E3-5* with the *openness* of 13.4%, 22.5%, 29.4%, 36.0%, and 41.5% respectively.

Evaluation metric. Following [19, 21, 29], we choose Area Under the Receiver Operating Characteristic (AUROC) as the evaluation metric of OSR. The corresponding false positive rate and true positive rate are calculated based on multiple thresholds, and these indexes are used as the horizontal and vertical values to draw the ROC curve. AUROC reflects the performance of a classifier by the area between the ROC curve and the coordinate axis. The value of AUROC ranges within [0, 1], and a larger AUROC score indicates better performance of the open-set classifier.

Implementation details. We maintain one prototype in each class as suggested in [17]. γ is set to 1.0, and α and β are set to 0.1. The classifier consists of 9 continuous 3×3 convolution layers, batch normalization (BN), and LeakyReLU. During training, the batch size is 64, and the classifier is trained with the momentum stochastic gradient descent (Momentum SGD) optimizer with the learning rate starting from 0.1 and decreasing by 0.1 times every 30 epochs, with a total of 100 training epochs. The generator converts a 100-dimensional latent representation into the 44×44 image through 4 continuous 4×4 deconvolutions along with Batch Normalization (BN) and ReLU. The discriminator consists of 4 continuous 4×4 convolution layers, Batch Normalization (BN), and LeakyReLU. The generator and discriminator are trained by the Adam optimizer with a learning rate of 0.0002.

The results in TABLE II-V report the averaged close-set accuracy (%) and open-set AUROC score (%) over five times of the 5-fold cross-validation. The best and the second best models are highlighted in bold and underlined, respectively. From TABLE II, the models trained on the data with the same three classes perform differentially on the test set containing a different number of unknown classes. For example, the open-set AUROC score of Softmax in the *E5-1* is 97.20%, while it drops sharply to 82.75% in the *E5-3* set. This may be caused by the increased number of unknowns in the test set, leading to the expansion of *openness* and high difficulty for OSR. Moreover, the unknowns from the *E5-3* data setting are *M2*, *M7*, and *M8*, while the Dunn index between *M7* and some classes in the training set (*M1*, *M4*, and *M5*) is less than 3, determining their hard separability. This means that M7, as an unknown class, is easily classified into known similar classes with a high degree of confidence. A similar situation also appears in the setting of experiments *E4* and *E5*. Obviously, from TABLE II and TABLE III, with the gradual increase of *openness*, the open-set AUROC score on the baseline Softmax shows a downward trend on the whole, especially in the *E3-5* experimental setting, the AUROC score is only 69.22%. The performance of the proposed OpenMR is superior to other models, with the AUROC score of 91.62% in the *E3-5*, a significant 23% improvement from baseline. In contrast, GCPL has a lower AUROC score than OpenMR in multiple experiments. This means that the synthesis of open-set examples helps the model to reconstruct the virtual unknown space during training, forcing the model to widen the margin among known and unknown classes.

TABLE II. OPEN-SET RECOGNITION PERFORMANCE OF DIFFERENT METHODS TRAINED ON BATCH 1 DATA WITH 5 KNOWN CLASSES

Methods	The close-set accuracy			The open-set AUROC score		
	E5-1	*E5-2*	*E5-3*	*E5-1 (8.7%)*	*E5-2 (16.1%)*	*E5-3 (21.6%)*
Softmax	99.90±0.07	99.92±0.03	99.98±0.01	97.20±1.08	98.68±0.36	82.75±0.54
OSRCI [19]	99.81±0.11	99.87±0.09	99.96±0.01	**99.64±0.24**	98.31±0.54	95.18±0.48
RPL [30]	99.99±0.01	99.99±0.01	99.99±0.01	99.52±0.11	99.25±0.11	91.78±0.80
GCPL [17]	99.94±0.04	99.93±0.04	99.99±0.01	98.35±1.00	99.18±0.49	94.02±0.81
OpenMR(Ours)	99.93±0.04	99.94±0.03	99.99±0.01	98.95±0.62	**99.35±0.35**	**95.26±0.67**

TABLE III. OPEN-SET RECOGNITION PERFORMANCE OF DIFFERENT METHODS TRAINED ON BATCH 1 DATA WITH 4 KNOWN CLASSES

Methods	The close-set accuracy				The open-set AUROC score			
	E4-1	*E4-2*	*E4-3*	*E4-4*	*E4-1 (10.6%)*	*E4-2 (19.4%)*	*E4-3 (25.8%)*	*E4-4 (30.9%)*
Softmax	100±0.00	99.99±0.01	99.99±0.01	100±0.00	98.92±0.38	99.45±0.31	**98.04±0.73**	86.84±0.39
OSRCI [19]	99.94±0.05	99.94±0.04	99.96±0.02	99.97±0.02	99.45±0.21	97.18±0.64	94.91±1.73	92.45±0.48
RPL [30]	100±0.00	100±0.00	100±0.00	100±0.00	99.48±0.12	99.47±0.18	97.73±0.89	91.04±1.15
GCPL [17]	100±0.00	100±0.00	99.99±0.01	100±0.00	98.33±0.95	98.98±0.39	97.97±0.90	93.46±0.85
OpenMR(Ours)	100±0.00	100±0.00	100±0.00	100±0.00	**99.52±0.32**	**99.48±0.21**	97.98±0.83	**94.65±0.50**

TABLE IV. OPEN-SET RECOGNITION PERFORMANCE OF DIFFERENT METHODS TRAINED ON BATCH 1 DATA WITH 3 KNOWN CLASSES

Methods	The close-set accuracy					The open-set AUROC score				
	E3-1	*E3-2*	*E3-3*	*E3-4*	*E3-5*	*E3-1 (13.4%)*	*E3-2 (22.5%)*	*E3-3 (29.4%)*	*E3-4 (36.0%)*	*E3-5 (41.5%)*
Softmax	100±0.00	100±0.00	100±0.00	100±0.00	100±0.00	98.43±0.17	97.30±0.23	98.36±0.07	84.50±1.55	69.22±0.28
OSRCI [19]	100±0.00	99.96±0.03	99.93±0.06	100±0.00	99.96±0.03	98.22±0.93	96.44±0.34	97.01±0.27	95.06±0.60	91.57±0.80
RPL [30]	100±0.00	100±0.00	100±0.00	100±0.00	100±0.00	**100±0.00**	99.70±0.07	99.66±0.05	90.10±0.71	85.90±0.72
GCPL [17]	100±0.00	100±0.00	100±0.00	100±0.00	100±0.00	**100±0.00**	99.58±0.18	99.74±0.07	91.60±1.04	89.88±0.49
OpenMR (Ours)	100±0.00	100±0.00	100±0.00	100±0.00	100±0.00	**100±0.00**	**99.99±0.00**	**99.87±0.02**	**95.35±0.42**	**91.62±0.59**

TABLE V. OPEN-SET RECOGNITION PERFORMANCE ON BATCH 2 DATA

Methods	The open-set AUROC score		
	E4-4 (30.9%)	*E3-4 (36.0%)*	*E3-5 (41.5%)*
Softmax	66.84±0.95	72.70±0.22	57.87±0.37
OSRCI [19]	80.99±1.16	78.90±1.44	70.73±1.23
RPL [30]	75.61±0.54	81.75±0.41	67.41±0.44
GCPL [17]	76.89±1.32	79.43±0.29	64.37±0.31
OpenMR(Ours)	**81.64±0.90**	**82.50±0.89**	**71.29±0.70**

To compare the OSR performance of multiple models more comprehensively, we choose the same experimental setting with an *openness* greater than 30% on the data of *Batch* 2 whose exploratory motion is changed from press to slide. From TABLE V, the open-set AUROC score on baseline Softmax decreased overall compared to that of *Batch* 1 data, especially in the *E3-5* experimental setting, the AUROC score only reaches 57.87%. And the performance of OpenMR is still superior to other models, with an increase of more than 10% over the baseline open-set AUROC score. This verifies the robustness of the proposed model on the detection of unknown classes again, but it is worth noting that the difficulty of OSR is increased under the change of external conditions such as exploration motion. Under the *E3-5* experimental setting, the open-set AUROC score of OpenMR only reaches 71.29%. In addition, when there are multiple types of unknown materials in the test environment, split different types still relies on manual labeling, which remains to be further improved.

VI. CONCLUSIONS AND FUTURE WORK

We discuss the open set tactile material recognition problem under different degrees of *openness*, and design the Open set Material Recognition (OpenMR) based on General Convolutional Prototype Learning (GCPL) to identify the unknown classes. The proposed method achieves high open-set recognition performance while maintaining great discriminative ability in the close-set classification. It is a preliminary attempt for robot tactile material recognition toward the open world. There remains the distortion problem of the generated open-set examples in some cases, which may reduce the unknown detection performance. In the future, we will try to further improve unknown class detection and automatic labeling for novel classes to aid the autonomous learning of robots in complex environments.

REFERENCES

[1] T. Lesort, V. Lomonaco, A. Stoian, D. Maltoni, D. Filliat, and N. Díaz-Rodríguez, "Continual learning for robotics: Definition, framework, learning strategies, opportunities and challenges," *Information fusion,* vol. 58, pp. 52-68, 2020.

[2] C. X. Geng, S. J. Huang, and S. C. Chen, "Recent Advances in Open Set Recognition: A Survey," *IEEE TRANSACTIONS ON PATTERN ANALYSIS AND MACHINE INTELLIGENCE,* vol. 43, no. 10, pp. 3614-3631, OCT 1 2021, doi: 10.1109/TPAMI.2020.2981604.

[3] D. Bogdoll, M. Nitsche, and J. M. Zöllner, "Anomaly detection in autonomous driving: A survey," in *Proceedings of the IEEE/CVF conference on computer vision and pattern recognition*, 2022, pp. 4488-4499.

[4] M. Gunther, S. Cruz, E. M. Rudd, T. E. Boult, and Ieee, "Toward Open-Set Face Recognition," presented at the 2017 IEEE CONFERENCE ON COMPUTER VISION AND PATTERN RECOGNITION WORKSHOPS (CVPRW), 2017.

[5] R. Vareto, S. Silva, F. Costa, W. R. Schwartz, and Ieee, "Towards Open-Set Face Recognition using Hashing Functions," presented at the 2017 IEEE INTERNATIONAL JOINT CONFERENCE ON BIOMETRICS (IJCB), 2017.

[6] D. Miller, L. Nicholson, F. Dayoub, and N. Sünderhauf, "Dropout sampling for robust object detection in open-set conditions," in *2018 IEEE International Conference on Robotics and Automation (ICRA)*, 2018: IEEE, pp. 3243-3249.

[7] J. Zheng, W. Li, J. Hong, L. Petersson, and N. Barnes, "Towards open-set object detection and discovery," in *Proceedings of the IEEE/CVF Conference on Computer Vision and Pattern Recognition*, 2022, pp. 3961-3970.

[8] W. Bao, Q. Yu, and Y. Kong, "OpenTAL: Towards Open Set Temporal Action Localization," in *Proceedings of the IEEE/CVF Conference on Computer Vision and Pattern Recognition*, 2022, pp. 2979-2989.

[9] H. Zhang, H. H. Ding, and Ieee, "Prototypical Matching and Open Set Rejection for Zero-Shot Semantic Segmentation," presented at the 2021 IEEE/CVF INTERNATIONAL CONFERENCE ON COMPUTER VISION (ICCV 2021), 2021.

[10] B. J. Meyer and T. Drummond, "The importance of metric learning for robotic vision: Open set recognition and active learning," in *2019 International Conference on Robotics and Automation (ICRA)*, 2019: IEEE, pp. 2924-2931.

[11] S. S. Baishya and B. Bäuml, "Robust material classification with a tactile skin using deep learning," in *2016 IEEE/RSJ International Conference on Intelligent Robots and Systems (IROS)*, 2016: IEEE, pp. 8-15.

[12] M. Kaboli and G. Cheng, "Robust tactile descriptors for discriminating objects from textural properties via artificial robotic skin," *IEEE Transactions on Robotics,* vol. 34, no. 4, pp. 985-1003, 2018.

[13] T. Taunyazov, H. F. Koh, Y. Wu, C. Cai, and H. Soh, "Towards effective tactile identification of textures using a hybrid touch approach," in *2019 International Conference on Robotics and Automation (ICRA)*, 2019: IEEE, pp. 4269-4275.

[14] T. Taunyazov, Y. Chua, R. Gao, H. Soh, and Y. Wu, "Fast Texture Classification Using Tactile Neural Coding and Spiking Neural Network," in *2020 IEEE/RSJ International Conference on Intelligent Robots and Systems (IROS)*, 2020: IEEE, pp. 9890-9895.

[15] S. Sankar *et al.*, "Texture discrimination using a flexible tactile sensor array on a soft biomimetic finger," in *2019 IEEE SENSORS*, 2019: IEEE, pp. 1-4.

[16] G. Cao, Y. Zhou, D. Bollegala, and S. Luo, "Spatio-temporal attention model for tactile texture recognition," in *2020 IEEE/RSJ International Conference on Intelligent Robots and Systems (IROS)*, 2020: IEEE, pp. 9896-9902.

[17] H.-M. Yang, X.-Y. Zhang, F. Yin, and C.-L. Liu, "Robust classification with convolutional prototype learning," in *Proceedings of the IEEE conference on computer vision and pattern recognition*, 2018, pp. 3474-3482.

[18] W. J. Scheirer, A. d. R. Rocha, A. Sapkota, and T. E. Boult, "Toward Open Set Recognition," *IEEE Transactions on Pattern Analysis and Machine Intelligence,* vol. 35, no. 7, pp. 1757-1772, 2013, doi: 10.1109/TPAMI.2012.256.

[19] L. Neal, M. Olson, X. Fern, W.-K. Wong, and F. Li, "Open set learning with counterfactual images," in *Proceedings of the European Conference on Computer Vision (ECCV)*, 2018, pp. 613-628.

[20] A. Bendale, T. E. Boult, and Ieee, "Towards Open Set Deep Networks," presented at the 2016 IEEE CONFERENCE ON COMPUTER VISION AND PATTERN RECOGNITION (CVPR), 2016.

[21] R. Yoshihashi, W. Shao, R. Kawakami, S. You, M. Iida, and T. Naemura, "Classification-reconstruction learning for open-set recognition," in *Proceedings of the IEEE/CVF Conference on Computer Vision and Pattern Recognition*, 2019, pp. 4016-4025.

[22] X. Sun, Z. Yang, C. Zhang, K.-V. Ling, and G. Peng, "Conditional gaussian distribution learning for open set recognition," in *Proceedings of the IEEE/CVF Conference on Computer Vision and Pattern Recognition*, 2020, pp. 13480-13489.

[23] D.-W. Zhou, H.-J. Ye, and D.-C. Zhan, "Learning placeholders for open-set recognition," in *Proceedings of the IEEE/CVF conference on computer vision and pattern recognition*, 2021, pp. 4401-4410.

[24] J. Jang and C. O. Kim, "Collective decision of one-vs-rest networks for open-set recognition," *IEEE Transactions on Neural Networks and Learning Systems,* 2022.

[25] P. Bevandić, I. Krešo, M. Oršić, and S. Šegvić, "Dense open-set recognition based on training with noisy negative images," *Image and Vision Computing,* vol. 124, p. 104490, 2022.

[26] Y. LeCun *et al.*, "Handwritten digit recognition with a back-propagation network," *Advances in neural information processing systems,* vol. 2, 1989.

[27] Y. Xie, C. Chen, D. Wu, W. Xi, and H. Liu, "Human-Touch-Inspired Material Recognition for Robotic Tactile Sensing," *Applied Sciences,* vol. 9, no. 12, p. 2537, 2019.

[28] J. C. Dunn, "Well-separated clusters and optimal fuzzy partitions," *Journal of cybernetics,* vol. 4, no. 1, pp. 95-104, 1974.

[29] K. Lee, H. Lee, K. Lee, and J. Shin, "Training confidence-calibrated classifiers for detecting out-of-distribution samples," *arXiv preprint arXiv:1711.09325,* 2017.

[30] G. Chen *et al.*, "Learning open set network with discriminative reciprocal points," in *European Conference on Computer Vision*, 2020: Springer, pp. 507-522.